Developmental Cell, Vol. 7, 731–743, November, 2004, Copyright ©2004 by Cell Press

γ-Secretase Functions through Notch Signaling to Maintain Skin Appendages but Is Not Required for Their Patterning or Initial Morphogenesis

Yonghua Pan,[1] Meei-Hua Lin,[1] Xiaolin Tian,[2] Hui-Teng Cheng,[1] Thomas Gridley,[3] Jie Shen,[4] and Raphael Kopan[1,*]

[1]Department of Molecular Biology and Pharmacology
Division of Dermatology
Department of Medicine
[2]Department of Genetics
Washington University School of Medicine
Box 8103
660 South Euclid Avenue
St. Louis, Missouri 63110
[3]The Jackson Laboratory
Bar Harbor, Maine 04609
[4]Center for Neurologic Diseases
Brigham and Women's Hospital
Program in Neuroscience
Harvard Medical School
Boston, Massachusetts 02115

Summary

The role of Notch signaling during skin development was analyzed using *Msx2-Cre* to create mosaic loss-of-function alleles with precise temporal and spatial resolution. We find that γ-secretase is not involved in skin patterning or cell fate acquisition within the hair follicle. In its absence, however, inner root sheath cells fail to maintain their fates and by the end of the first growth phase, the epidermal differentiation program is activated in outer root sheath cells. This results in complete conversion of hair follicles to epidermal cysts that bears a striking resemblance to Nevus Comedonicus. Sebaceous glands also fail to form in γ-secretase-deficient mice. Importantly, mice with compound loss of *Notch* genes in their skin phenocopy loss of γ-secretase in all three lineages, demonstrating that Notch proteolysis accounts for the major signaling function of this enzyme in this organ and that both autonomous and nonautonomous Notch-dependent signals are involved.

Introduction

The skin is an essential organ protecting the organism from invasion of pathogens and chemicals and preventing the escape of liquids and nutrients. The initial step in skin morphogenesis is a transition from simple epithelium, the embryonic ectoderm, to a stratified epithelium. Next, the Wnt pathway and the TNFα-related ectodermal dysplasia receptor (EDAR) participate in a series of inductive events orchestrating the separation of the hair lineages from the epidermal lineage (reviewed in Alonso and Fuchs, 2003; Fuchs and Raghavan, 2002; Millar, 2002; Stenn, 2003). Despite renewed interest, the origin of the sebaceous gland lineage has not been defined (Allen et al., 2003; Nichols et al., 2004; Niemann et al., 2003).

Mature mouse hair follicles are highly organized structures, symmetrical about a proximo-distal axis (Figure 1A). At the center of the follicle is the hair shaft, comprised of the medulla, cortex, and hair cuticle cells. The hair shaft is encircled by the inner root sheath (IRS) cells. The outer root sheath (ORS) is a stratified epithelium that is contiguous with the epidermis and separated from the IRS by the companion layer. Two protruding structures adjacent to the upper ORS are the sebaceous gland, which synthesizes and secretes the lipid droplets (sebum) into the hair canal, and the bulge, a stem cell niche, defined by slow-cycling and label-retaining cells (Braun et al., 2003; Taylor et al., 2000; Tumbar et al., 2004). The bulb (most proximal structure) contains undifferentiated, proliferating matrix cells, which engulf a small cluster of specialized mesenchymal cells called Dermal Papilla (DRP). The adult hair follicles cycle between growth (anagen), degeneration (catagen), and rest (telogen), while the sebaceous glands and the structures above the bulge region remain relatively stable. The interfollicular epidermis alters gene expression and homeostatic control (thickness) in response to mechanical stimuli and wound healing (Sengel, 1976). ORS cells can replenish the epidermis after injury, reflecting a built-in flexibility permitting a switch between these two fates.

Notch signaling is involved in a variety of cell-fate decisions in all metazoans. Mutations affecting components of this pathway cause several human disorders (Gridley, 2003) and can either promote or suppress cancer (Weng and Aster, 2004). In response to ligand binding, Notch proteins (e.g., Notch 1-4 in the mouse) are sequentially cleaved by two proteases: a metalloprotease sheds the extracellular portion of the Notch receptor, and then γ-secretase hydrolyzes a peptide bond within the transmembrane domain. As a result, the Notch intracellular domain (NICD) dissociates from the membrane and enters the nucleus, where it directly interacts with the DNA binding protein RBPjk. This interaction displaces the corepressor complex that is associated with RBPjk under basal conditions, leading to assembly of a transcriptionally active complex (Lubman et al., 2004).

Notch pathway molecules are expressed in the skin and the hair follicle (Favier et al., 2000; Kopan and Weintraub, 1993; Lin and Kopan, 2003; Powell et al., 1998; Yamamoto et al., 2003). Several distinct functions for Notch signaling in skin have been proposed. (1) Control of proliferation/commitment/differentiation decisions in the epidermis or in keratinocytes differentiating in culture that require Notch1 to induce p21 and caspase3 (Nicolas et al., 2003; Okuyama et al., 2004; Rangarajan et al., 2001). Surprisingly, both loss (Nicolas et al., 2003) and overexpression (below and Lin and Kopan, 2003) of Notch1 promote proliferation in stratified epithelia, suggesting a complex role for Notch in controlling epidermal homeostasis. (2) Regulation of the stem cell niche in the epidermis and regulation of differentiation choices in the bulge where loss of *RBPjk* promoted

*Correspondence: kopan@wustl.edu

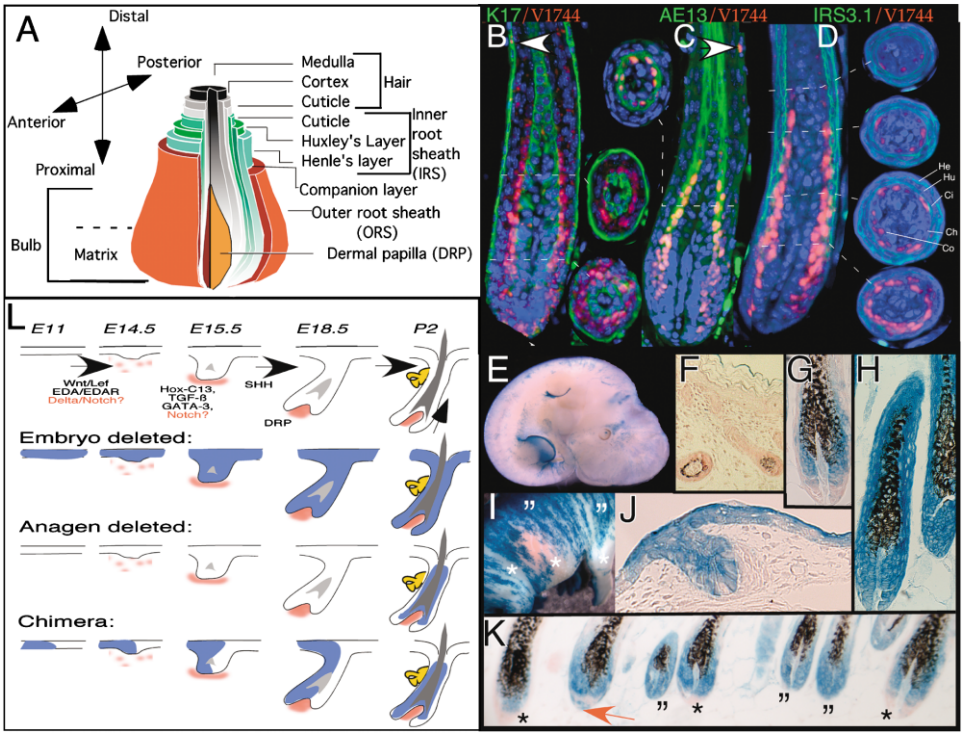

Figure 1. The Expression Domain of *Msx2-Cre* Generates Hair Follicles with Three Distinct Patterns of Gene Loss

(A) Schematic diagram of the organization and composition of the hair follicle.

(B–D) Double immunofluorescence staining of wild-type P8 follicles with Val1744 antibody and antibodies against hair cell-type-specific markers: K17 (medulla and ORS), AE13 (cortex [Co] and cuticle [Ch]), and IRS 3.1 (Henle's [He], Huxley's [Hu], and cuticle [Ci]). Dotted line marks the approximate position of each cross-section along the proximo-distal axis.

(E–K) X-gal staining of (*Msx2-Cre*/+; *ROSA26R*/+) embryos and skin sections. Embryos at E11.5 (E) and E15.5 (I), and skin sections at E15.5 (J), P0 (F), and P8 (G, H, K).

(L) Diagram of gene loss patterns generated by *Msx2-Cre*. In the top row, the stage and signaling molecules thought to regulate hair morphogenesis are indicated. Blue color indicates the gene deletion patterns shown by X-gal staining.

entry into the epidermal instead of the follicular program (Lowell et al., 2000; Yamamoto et al., 2003). (3) Patterning of epithelial appendages (Chen et al., 1997; Crowe et al., 1998). (4) A non-cell-autonomous role of Notch1 in regulating the medulla (Lin et al., 2000) and perhaps the epidermis (Lin and Kopan, 2003). However, interpretation of Notch function in these studies was inherently limited because the conclusions were derived from studies involving cultured cells, overexpression of activated Notch1 proteins, or removal of Notch1 signaling either postnatally (*Notch1*) and/or in only a fraction of cells (*Notch1* and *RBPjk*).

To systematically analyze the contribution of Notch signaling to the patterning and differentiation of mouse skin, we used the Cre-LoxP system (Sauer and Henderson, 1988) to remove multiple Notch alleles individually or in combination, as well as all of Notch signaling by removal of γ-secretase (i.e., both presenilin genes, *PS1* and *PS2* [Saura et al., 2004]). Cre was expressed in the primitive ectoderm using *Msx2* minimal promoter that is active in the apical ectodermal ridge (AER) and the basal embryonic ectoderm at E9.5 (Sun et al., 2000). This promoter is also active later in the developing hair follicle (Kulessa et al., 2000). Our results indicate that Notch signaling plays multiple and distinct roles in the three epithelial skin lineages. In contrast to the roles played by the Notch pathway in tissues analyzed thus far, loss of γ-secretase (and thus Notch signaling) did not affect skin patterning nor did it affect cell fate selection or early differentiation within the follicle. Instead, it resulted in follicular atrophy in part due to the failure of IRS cells to maintain their differentiated cellular identity within the follicle. Initiation of catagen triggered conversion of ORS cells into epidermal cysts that closely resemble Nevus Comedonicus, a benign form of acne often associated with other developmental abnormalities. The epidermis and the ORS were severely hyperplasic and the sebaceous glands were missing. Loss of *Notch1* in the embryonic ectoderm affected epidermal differentiation only mildly; however, in hair follicles, non-cell-autonomous defects were detected in the medulla and the IRS, reminiscent of the consequences of gain of *Notch1* function in the cortex. Importantly, compound loss of *Notch1* and *2* phenocopied loss of γ-secretase in the follicle and sebaceous gland and loss of *Notch1, 2,* and *3* phenocopied loss of γ-secretase in the epidermis, suggesting that Notch proteins are the major mediators of γ-secretase function in the skin.

Results

The Pattern of Notch1 Activation in the Hair Follicles Is Consistent with a Role in Lateral Inhibition or Fate Induction

We have previously described the distribution of NICD in the epidermis and the hair follicle using the Val1744

antibody, which recognizes the new epitope on activated Notch1 generated by γ-secretase cleavage (Cheng et al., 2003; Lin and Kopan, 2003; Schroeter et al., 1998). To identify the cells containing NICD, we examined the colocalization of hair cell-type-specific markers and Val1744 on skin sections from wild-type animals (Figures 1B–1D). The majority of NICD-containing cells were located in the cortex and the hair cuticle in MHKA-1-expressing cells (AE13-positive; Figure 1C). In addition, we found a few NICD-containing cells in the K17-expressing ORS (arrow in Figures 1B and 1C) and in the cuticle layer of the IRS (IRS 3.1-positive; Figure 1D). NICD was not detected in the differentiating medulla (K17-positive; Figure 1B) or in cells adjacent to the DRP. The NICD-positive cells in the matrix were not labeled by any of the markers. This pattern suggests that Notch signaling may mediate cell fate selection within the bulb, either by inhibiting cells from acquiring noncortex fates or by directly inducing the cortex differentiation program.

Msx2-Cre-Mediated Deletion Generates Hair Follicles with Three Distinct Patterns of Gene Loss

To examine the role of Notch signaling during skin morphogenesis, we chose to perform targeted deletion of Notch pathway genes prior to onset of patterning event. Since Notch was proposed to retain skin stem cells (Lowell et al., 2000) and to be essential for epidermal differentiation (Rangarajan et al., 2001), we wished to avoid postnatal lethality predicted to occur with complete loss of Notch signaling in all keratinocytes. We thus selected the *Msx2-Cre* transgenic line due to its early (E9.5) and restricted expression within the embryonic ectoderm (Barrow et al., 2003; Meyers et al., 1998; Sun et al., 2000). To precisely characterize Cre activity in the skin, we analyzed the reporter *Msx2-Cre/+; ROSA26R/+* double transgenic mice in which LacZ expression is blocked by a floxed "stop" cassette (Soriano, 1999). To directly examine Cre expression, we used anti-Cre antibodies. Ectopic, ectodermal Cre expression resulted in restoring *LacZ* expression at the dorsal midline. As embryos develop, LacZ-positive areas expanded laterally (Figure 1E, E11.5; Figure 1I, E15.5) either by clonal expansion or by progressive expression of *Cre* at later ages. We could not detect Cre protein at E14.5, consistent with the possibility that some clonal expansion occurs. Since the cues separating the epidermal lineage from the hair germ may act dorsally around E13 (Andl et al., 2002; Millar, 2002), the early dorsal deletion (at E9.5) allows us to evaluate the contribution of any particular gene to this process. While hair follicles were predicted to develop normally in areas where *Cre* was never expressed (white in Figures 1F and 1I, asterisk), follicles developing in the dorsal cells where *Cre* expression commenced at E9.5 (blue in Figures 1H, 1I", and 1J) were predicted to have lost all gene expression in homozygously floxed lines and thus referred to as *embryo-deleted* follicles. A second phase of *Cre* expression was initiated in the matrix of every follicle at P1, just below the widest diameter (line of Auber; Figure 1G and Supplemental Figure S1 at http://www.developmentalcell.com/cgi/content/full/7/5/731/DC1/), similar to the normal *Msx2* expression domain during anagen (Kulessa et al., 2000; Ma et al., 2003). Follicles that only experienced this second phase of Cre expression were referred to as *anagen-deleted* follicles. Importantly, up to 10 proximal bulb cells in *anagen-deleted* follicles did not express Cre and thus remained LacZ negative during anagen; sebaceous glands, ORS, and interfollicular epidermal cells were likewise devoid of Cre activity in these areas. Finally, because each coat-hair has a polyclonal origin (Kopan et al., 2002; Mintz, 1971; Mintz and Silvers, 1970), *chimeric* follicles would form at the boundary of *Msx2-Cre*-positive and -negative territories during development (Figure 1K, red arrow). These follicles contained cells that arose from both *embryo-deleted* and *anagen-deleted* progenitors and could be used to assess nonautonomous effects of gene products. The patterns of gene loss are summarized in Figure 1L.

The expression pattern of *Msx2-Cre* facilitates the analysis of a skin phenotype. Most of the hair growth is accomplished after P4, a time when every *embryo-deleted* follicle has lost floxed genes in all cells. However, in *anagen-deleted* follicles, mRNA levels and protein half-life would actually determine how soon cells become depleted for the protein along the proximodistal axis. Therefore, if a protein plays an essential role in the distal part of the hair follicle, *embryo-deleted*, *anagen-deleted*, and *chimeric* follicles would all have identical phenotypes after P4; only the distal tip of *anagen-deleted* hairs would be expected to maintain wild-type appearance because *Cre* expression was initiated after this segment of the follicle developed (P1, Figure 1F). In contrast, if a protein functions in the proximal part of the hair follicle, only *embryo-deleted* follicles would be expected to display the loss-of-function phenotypes. Chimeric follicles may show an intermediate proximal phenotype; however, given that up to four multipotent progenitors can contribute to one follicle (Kopan et al., 2002), different proportions of *Cre*-expressing cells would contribute to chimeric follicles, making data analysis too complex. We therefore chose to focus our studies primarily on the *embryo-* and *anagen-deleted* follicles.

A Differentiated Phenotype Cannot Be Maintained in γ-Secretase-Deficient Follicles

To avoid obscuring a phenotype due to compensation and redundancy among the four Notch receptors, we began our analysis by targeting γ-secretase, the enzyme essential for releasing NICD from all Notch proteins (Mizutani et al., 2001; Saxena et al., 2001). The catalytic site of γ-secretase resides in PS proteins. *PS2*-deficient mice have no phenotype; *PS1*-deficient mice die in utero (Herreman et al., 1999). To assess the role of γ-secretase in skin development, we thus generated mice with the genotype $PS1^{flox/flox}$; $PS2^{-/-}$; *Msx2-Cre/+* (referred to as PSDCKO [Saura et al., 2004]). PSDCKO mice were homozygous null for PS2 in all tissues and were also homozygous null for PS1 within the *Msx2-Cre* expression domain. The postnatal hair follicles in PSDCKO skin thus lack γ-secretase activity in either all cells (*embryo-deleted*) or only in cells above the line of Auber (*anagen-deleted*).

$PS1^{flox/flox}$; *PS2/+*; *Msx2-Cre/+* mice showed a transient phenotype in *embryo-deleted* skin (Figure 2B, asterisk), but by P22 had developed a normal coat (Figure 2B′) with a few abnormal looking follicles (similar to PSDCKO, see below). In contrast, the PSDCKO mice were smaller than littermates by P12 and had naked skin patches that became scaly and thick (Figures 2B′

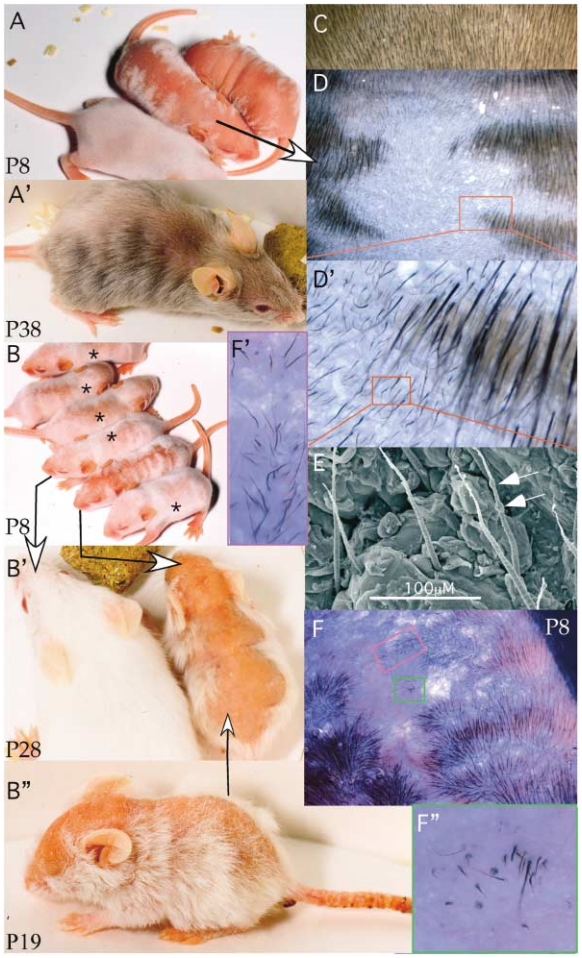

Figure 2. Skin Phenotypes in Mutant Mice and Their Littermates

(A and A′) N1CKO

(B–B″) PSDCKO. Asterisks in (B) identify PS1CKO; PS2/+ pups.

(C–F) Light microscopy of wild-type (C), N1CKO (D, D′), and PSDCKO (F–F″) skin at P8. Images in (D), (D′), and (E) are progressively magnified, as are (F), (F′), and (F″). (E) Scanning electron microscopy (SEM) of N1CKO skin. Age indicated on the images.

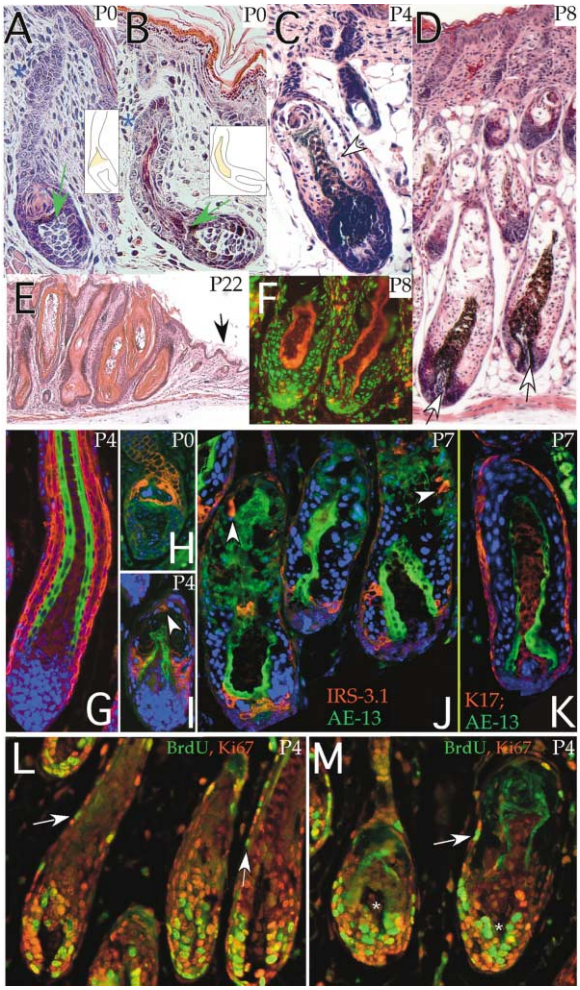

Figure 3. Histological and Immunohistochemical Analysis of *embryo-deleted* PSDCKO Skin

(A–E) H&E staining of hair follicles at the indicated ages. PSDCKO (A) and wild-type hair follicle (B) at P0. Note the progressive deterioration of follicles with increasing age (A–E). Follicles eventually convert to cysts (E, arrow; skin in telogen).

(F) The degenerating hair follicles lack nuclear Val1744 immunoreactivity, confirming lack of γ-secretase activity (DAPI staining in green). Nonspecific red staining is detected around the degenerating hair shafts.

(G–J) Normal cell fate specification in the absence of γ-secretase as revealed by double immunofluorescence at the indicated ages. Wild-type P4 hair follicle (G) is compared to *embryo-deleted* follicles from PSDCKO mutant skin patch [(G–K), DAPI in blue; (G–J), IRS3.1 (red)/AE13 (green); (K), K17 (red)/AE13 (green)]. Note decline in IRS3.1-positive cells and their disassociation from each other (arrowheads).

(L and M) BrdU (green) and Ki67 (red) double immunofluorescence staining of the *anagen-deleted* (L) and *embryo-deleted* follicles (M) from the same PSDCKO mice (BrdU labeling for 1–2 hr).

and 2B″). PSDCKO mice died after weaning (the longest survivor died at P30), most likely from hyperplasia of the esophagus (not shown). The short postnatal period not withstanding, we identified three regions in skins of PSDCKO animals that differed in their morphology (Figure 2F). Regions bearing normal hairs (presumably *anagen-deleted*) and naked territories (presumably *embryo-deleted*; Figure 2F″) were separated by regions covered with short hairs that could be chimeric follicles (Figure 2F′). The assignment of the shorter hairs as *embryo-deleted* was confirmed by X-gal staining of *PSDCKO; ROSA26R*/+ skin (not shown) or by Val1744 antibody staining (Supplemental Figure S2).

The naked skin regions of PSDCKO mice were initially thought to indicate a role for Notch signaling in hair patterning. Histological examination of PSDCKO skin, however, revealed that hair follicles formed with normal periodicity even in the dorsal midline *embryo-deleted* territory (which expresses Cre at E9.5; Figure 3A and Supplemental Figure S3). To assure ourselves that Notch signaling is not required for patterning, we examined the consequences of removing γ-secretase with another Cre transgene, *Pax6 (Le)-Cre*. This promoter is active early (E9.5) and uniformly in the eye primordia (including the surface ectoderm), removing floxed alleles from the developing eyelids, cornea, and the lens in a

large territory (Ashery-Padan et al., 2000). We analyzed the hair patterning in eyelids from *PSDCKO;Pax6(le)-Cre* mice and found them indistinguishable from wild-type eyelids at P0 (R. Rajagopal, Y.P., D. Beebe, and R.K., unpublished observation).

Normally, the interface between the apex of DRP and the epithelial cells assumes a teardrop shape at P0 with eosinophilic cells forming the hair shaft (Figure 3B, arrow). In PSDCKO follicles, an epithelial cluster forms an unusual flat boundary with the DRP in the *embryo-deleted* follicles (Figure 3A, arrow). At P4, the upper part of the *embryo-deleted* hair follicles contained loosely packed cells with enlarged cytoplasm and small nuclei (Figure 3C, arrow); melanin-containing cells, a characteristic feature of the differentiating hair shaft (Slominski et al., 1991), were still detected in the abnormal hair structure. The loosely packed cells extended farther down to the matrix at P8, leaving the ORS and the DRP as the only discernible hair structures; all other cell layers appeared to have collapsed around the melanin-containing core (Figures 3C and 3D). At P12 and more obviously at P15 (catagen), the degenerating follicles lost contact with their DRP (which could still be identified by morphological criteria and alkaline phosphatase [AP] staining [not shown]) and the ORS had begun to proliferate, stratify, and keratinize (Figure 3E). By P22, keratinized cysts had replaced the *embryo-deleted* hair follicles, while the adjacent *anagen-deleted* section was in telogen (Figure 3E). Throughout all stages, degenerating follicles contained no evidence for NICD immunoreactivity, a marker for γ-secretase activity; recognizable follicles on the same section contained at least some cells with NICD (Figure 3F and Supplemental Figure S2). The postnatal hair phenotypes of *PSDCKO;Pax6(le)-Cre* and *PSDCKO;Msx2-Cre* were indistinguishable. This observation indicates a profound dependence on γ-secretase for completion, but not initiation, of hair morphogenesis.

Loss of γ-Secretase Does Not Impair Proper Allocation of Cell Fates

If γ-secretase contributes to cell fate acquisition within the follicle, we presumed that in its absence, some cell type(s) would fail to form while others may expand. To determine the extent of cellular differentiation within the γ-secretase-deficient hair follicles, we examined the expression of markers for each follicular cell type. These included cortex/cuticle-specific MHKA-1 and S100A3 (Lin et al., 2000), GATA-3 (Kaufman et al., 2003), and IRS3.1, specific for IRS cells (Porter et al., 2004) and trichohyalin, which is expressed in the IRS and medulla (O'Guin et al., 1992). Surprisingly, cells positive for all markers were detected in γ-secretase-deficient follicles (Figures 3G–3K and not shown). The nested organization of cell layers was also preserved (IRS-cuticle-cortex-medulla-cortex-cuticle-IRS; Figures 3H–3K). However, IRS cells seemed to be severely affected: IRS 3.1-positive cells were born but contributed to a smaller fraction of the follicular census by P7 relative to the AE13-positive cortex or K17-positive medulla cells. A few IRS 3.1-positive cells could still be detected among the population of loosely packed cells occupying the space between the cortex and the ORS (Figures 3I and 3J, arrowheads). These loosely packed cells were GATA-3 negative (not shown) and were most likely derived from IRS cells that failed to maintain their differentiated state. The lack of IRS cells was not due to increase in apoptosis (based on TUNEL assay and distribution of activated Caspase3; data not shown), nor was it due to failure in proliferation within the bulb. BrdU incorporation at P4 was confined to the cells adjacent to the DRP (Figure 3M, asterisk) and to a few cells in the ORS (Figure 3M, arrow), similar to the labeling patterns of *anagen-deleted* follicles from the same animal (Figure 3L) or wild-type littermates (not shown). No BrdU or Ki67 labeling could be detected in the melanin-containing "core" or in the loosely packed cells of *embryo-deleted* PSDCKO follicles, indicating they are postmitotic. At P8, preference for labeling near the DRP remained, but fewer cells were labeled. From P12, more BrdU-labeled cells were detected in the ORS, and at a later stage (P15) this was accompanied by the stratification, keratinization, and cyst formation of follicles (not shown and see below).

Outer Root Sheath Cells from γ-Secretase-Deficient Follicles Revert to the Epidermal Program at the End of the First Anagen

To determine if the epidermal program was activated in the ORS at P12, sections of PSDCKO skin were stained for epidermal keratins (AE1) and the granular layer differentiation marker Filaggrin. Figure 4A illustrates the organization of these markers in wild-type epidermis. While the *embryo-deleted* epidermis at P8 was acanthotic and hyperkeratotic (Figures 4B, Supplemental Figure S3), the ORS was normal, comprised of a single layer of AE1-positive, Filaggrin-negative cells (Figures 4C, inset, and enlarged in 4D). However, at P12, hair follicle-derived cysts had begun expressing Filaggrin (Figures 4E and 4F). By P23, no recognizable follicles remained (Figure 4G).

Epidermal hyperproliferation, evident in PSDCKO epidermis, can be associated with inflammation (Tournoy et al., 2004). However, no staining was detected with antibodies against CD3 and CD45R by the time a phenotype was evident. In addition, histological evidence for an inflammatory response was observed in less than 20% of the P12–P25 PSDCKO sections we examined (not shown). Therefore, we concluded that the skin defects we observed in PSDCKO mice are a direct consequence of gene loss and not secondary to an inflammatory reaction.

An Essential Function for Notch1 in the Hair Bulb

Multiple substrates of γ-secretase have been reported (Kopan and Ilagan, 2004), raising the possibility that the consequences of γ-secretase loss can not be attributed exclusively to loss of Notch signaling. To determine the contribution of Notch signaling to the γ-secretase phenotype, we initiated the phenotypic analyses of single and compound *Notch* mutants in the skin. Mice homozygous for a conditional allele of Notch1 ($N1^{flox/flox}$) (Radtke et al., 1999; Yang et al., 2004) were bred to generate viable and fertile $N1^{flox/flox}$; *Msx2-Cre*/+ (N1CKO) mice. N1CKO pups were born at expected frequencies; as the first hair follicles emerged, a mosaic pattern of hair growth was detected and maintained throughout life

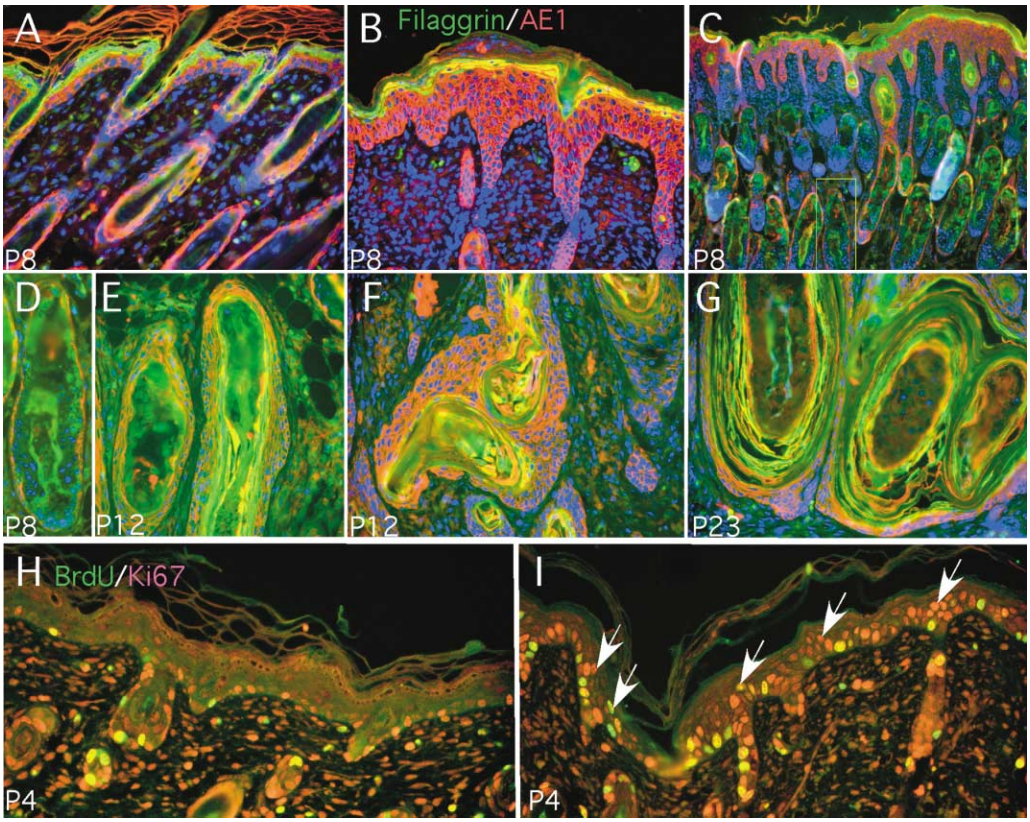

Figure 4. The ORS of *embryo-deleted* PSDCKO Follicles Reverts to Epidermal Program at the End of the First Anagen

(A–G) Immunofluorescence staining for epidermal markers AE1 (red) and Flaggrin (green) of wild-type (A) and PSDCKO *embryo-deleted* skin patch. DAPI in blue.

(H and I) BrdU (green) and Ki67 (red). Note that BrdU incorporation and Ki67 staining, normally confined to the basal layer (H), can be seen in suprabasal cells of PSDCKO mutant skin at higher frequency (arrows, I).

(Figures 2A and 2A′ and not shown). Only two hair morphologies were seen in N1CKO skin: finer, shorter, and wavy hairs (reminiscent of the chimeric hairs in the PSDCKO mice; Figure 2F′) that showed twisted, knotted morphology including bulbous perturbations in the shaft by scanning electron microscopy (SEM) (arrows in Figure 2E); the rest were indistinguishable from wild-type ones at both light microscopy and SEM levels (Figures 2D and 2D′ and not shown). Normal hair pattern was apparent in both territories (Figures 2A and 2A′ and Supplemental Figure S3). To confirm that wild-type hairs were *anagen deleted* and the shorter hairs as *embryo deleted*, we examined *N1CKO; ROSA26R/+* skin by whole-mount X-gal staining (not shown) and N1CKO follicles with Val1744 antibody. Follicles lacking NICD altogether (Figure 5H, blue arrow) were next to follicles with unilateral NICD staining (Figure 5H, red arrow).

Since both PSDCKO and N1CKO mice contained territories with normal hairs, *anagen-deleted* hairs must have had sufficient gene activity to complete follicular development while *embryo-deleted* and some *chimeric* follicles did not. These results are consistent with the possibility that γ-secretase and *Notch1* play a role in the proximal matrix of the hair follicle.

Notch1 Plays a Non-Cell-Autonomous Role in Hair Differentiation

N1CKO mice had properly patterned skin (Supplemental Figure S3); however, normal regions contained all four follicular types (Guard, Awl, Auchene, and Zigzag, not shown) while the aberrant morphology of the *embryo-deleted* follicles (Figures 2D and 2E) precluded us from identifying any hair types. To determine if alterations in cellular fates occurred in *embryo-deleted* N1CKO hairs, we examined expression of the markers used to analyze PSDCKO mice. Again, cells positive for each of these markers were detected (Figure 5 and not shown), but the overall follicular morphology was perturbed. Trichohyalin expression clearly demarcated the IRS and medulla in the *anagen-deleted* follicles (Figure 5A), but these layers appeared disorganized in the *embryo-deleted* follicles on the same section (Figure 5B). GATA-3, the IRS fate regulator, was expressed in N1CKO follicles (Figures 5F and 5G). The expression of K17 appeared normal in the ORS of P8 hair follicles but was drastically reduced in the medulla of *embryo-deleted* follicles from the same section (Figure 5D). To confirm this result, we extracted hair keratins from *embryo-deleted* and *anagen-deleted* hairs clipped from the same N1CKO mouse.

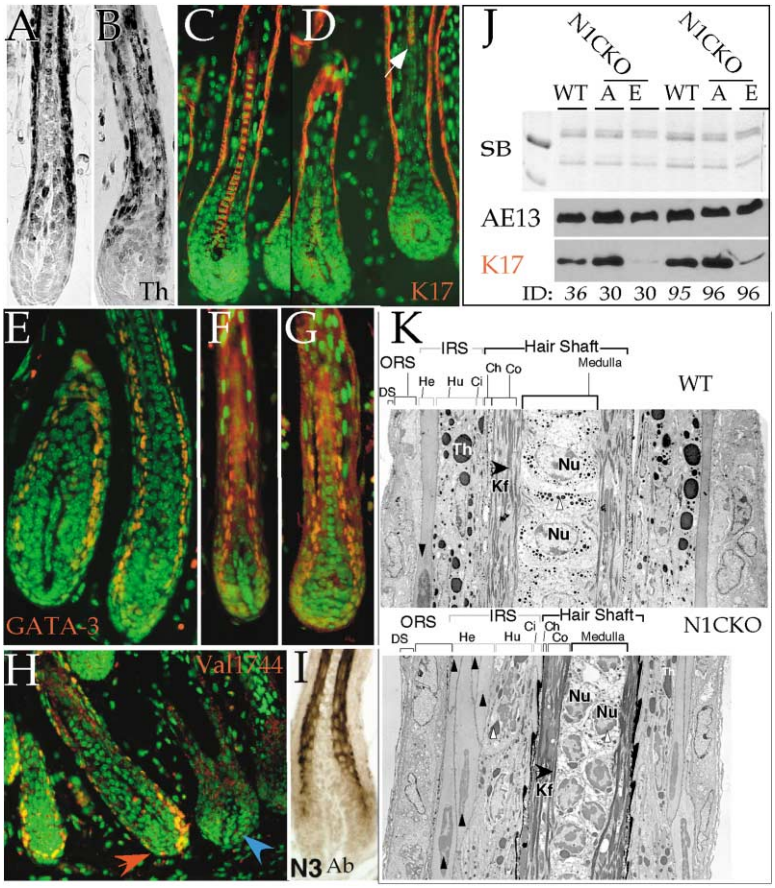

Figure 5. Notch1 Has a Non-Cell-Autonomous Role in Hair Bulb

(A and B) Trichohyalin staining (AE15, black).

(C–H) Immunofluorescence counterstained with DAPI (green). (C and D) K17 expression (red), arrow in (D) indicates reduced expression in the medulla; (E–G) GATA-3 staining (red) depicts IRS specification in wild-type (E), N1CKO (F), and N1CKO; MHKA-ΔE follicle (G). (H) NICD is visualized by Val1744 (red). Blue arrow marks an *embryo-deleted* follicle and red arrow marks a chimera.

(I) Notch3 expression in the distal follicle, brown.

(J) Western blot analysis of K17 expression in the hair shafts of *embryo-deleted* (E) and *anagen-deleted* (A) follicles from same N1CKO mice compared to wild-type littermates. Animal ID is indicated by number.

(K) Transmission election microscopic analysis of N1CKO *embryo-deleted* hair follicle and the follicle from wild-type littermate. Co, cortex; Ch, hair cuticle; Ci, IRS cuticle; Hu, Huxley's layer; He, Henle's layer; DS, dermal sheath; Nu, matrix nucleus; Th, Trichohyalin; Kf, keratin filaments.

The amounts of the cortical marker AE13 were unchanged; however, a dramatic reduction in K17 amounts was detected in the mutant hair follicles (Figure 5J).

To characterize *embryo-deleted* follicles further, transmission electron microscopic analysis (TEM) was conducted (Figures 5K and 5H). Instead of a single column of medulla cells with small trichohyalin granules below each nucleus, some sections contained two smaller cells packed inside the medulla with fewer, disorganized trichohyalin granules (Th; Figure 5K). In addition, the IRS Henle's layer (He; Figure 5K) was improperly organized: up to four cell tips could be seen in the mutant hair where normally only two cells overlapped (black arrowheads; Figure 5K). In contrast to these cell layers, the cortex appeared normal with clearly discernible keratin filaments (Kf; Figure 5K).

Embryo-deleted presenilin and *Notch1* Hair Follicles Lack Sebaceous Glands

Sebaceous gland precursors are recognized initially as a swelling in the upper ORS of the hair follicle, but no molecular markers exist to mark them at this stage. The mature sebaceous gland can be positively identified by using a lipophilic dye, Oil Red-O, or by immunohistochemistry with antibodies against the Stereoyl-CoA-Desaturase 1 (SCD1) (Heinemann et al., 2003; Zheng et al., 1999).

Morphologically, sebaceous glands seem to have formed as judged by the distinctive swelling in the upper ORS of *Notch1* (not shown) and *PS embryo-deleted* hair follicles (Figure 3A, asterisk). Oil Red-O and *SCD1* staining detected sebocytes after P1 in wild-type hair follicles (Figures 6A, 6C, and 6E). However, mature sebocytes were not detected in *embryo-deleted* hair follicles of PSDCKO (Figures 6F–6H). In contrast, we observed single, SCD1-positive cells in a few N1CKO follicles (Figure 6D).

Compound Notch Phenotypes: Deficiency of *Notch1* and *Notch2* Resembles Loss of γ-Secretase in Hair Follicle and Sebaceous Glands, while Loss of *Notch1, 2,* and *3* Resembles Defective γ-Secretase in Epidermis

Notch3 is expressed distally to Notch1 in the cortex (Figure 5I), in the epidermis, and in the sebaceous gland (not shown). *N3*-null mice are viable and normal (Krebs et al., 2003) with no skin phenotypes (Y.P. and R.K., not shown). Compound mutant mice (*$N1^{flox/flox}$; $N3^{-/-}$; Msx2-Cre* or N1N3CKO) displayed similar follicular morphologies to N1CKO (not shown).

Notch2 mRNA is present in the IRS precursors, distal to *Notch1*, and is retained in differentiated IRS cells (Figure 7A) and the epidermis (Rangarajan et al., 2001).

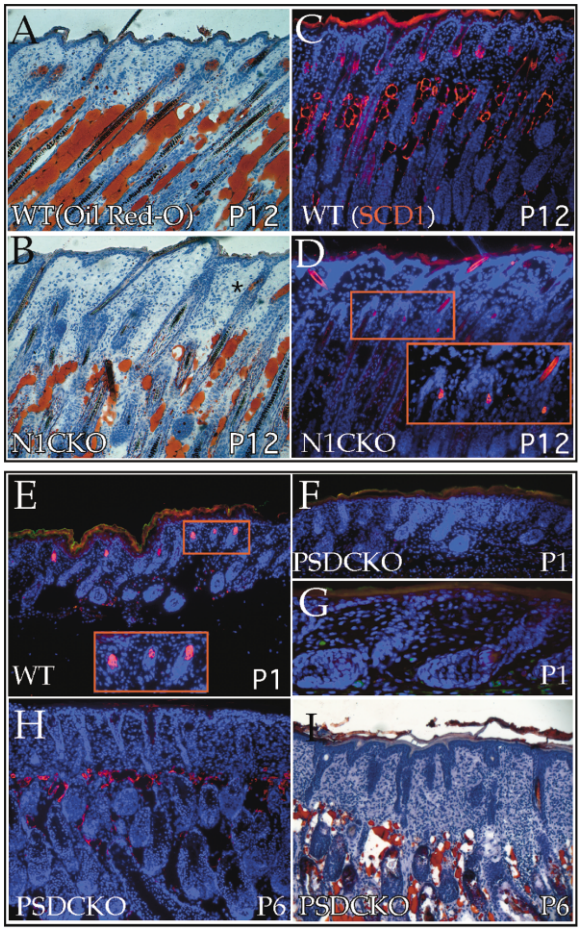

Figure 6. Sebaceous Glands Are Affected in N1CKO and Missing from PSDCKO *embryo-deleted* Skin

(A, B, and I) Oil Red-O staining of representative wild-type (A), *embryo-deleted* N1CKO (B), and PSDCKO (I) skin sections at indicated ages.

(C, D, E–H) Immunofluorescence detection of SCD1 (red) and DAPI (blue) counterstaining of wild-type (C and E), *embryo-deleted* N1CKO (D), and PSDCKO (F–H) skin sections at the indicated ages. (G) is a magnified view of (F). Insets in (D) and (E) are the magnified view of boxed regions. P6 wild-type skin (not shown) is identical to P12 skin (A and C).

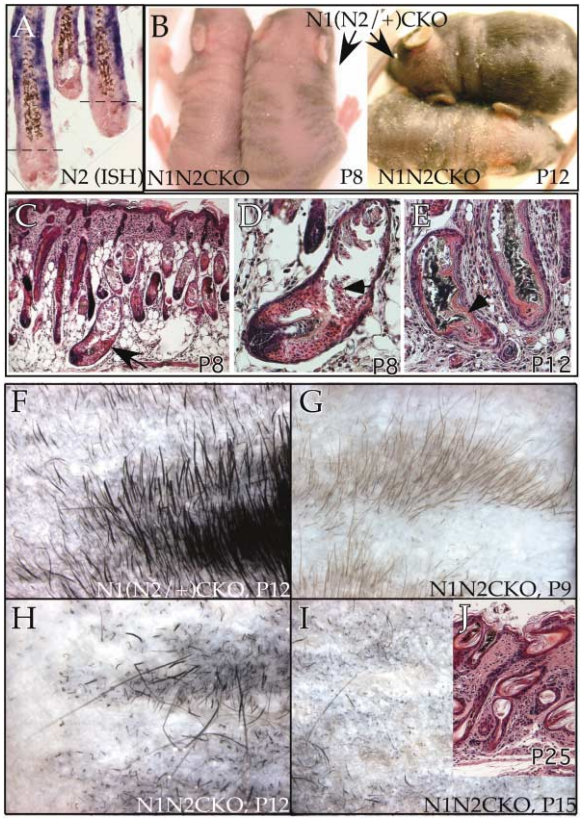

Figure 7. *embryo-deleted* N1N2CKO Follicles Phenocopy PSDCKO Follicles while *anagen-deleted* N1N2CKO Follicles Have an Intermediate Phenotype

(A) ISH for Notch2 reveals distal expression in IRS.

(B) N1N2CKO with a Notch2 heterozygous littermate (N1(N2/+)CKO) at indicated ages.

(C–E) Histological examination of H&E stained *embryo-deleted* N1N2CKO follicles.

(F–I) Magnified view of dorsal skin reveals progressive loss of hair in the *anagen-deleted* regions of N1N2CKO mice.

(J) H&E stained section of *anagen-deleted* N1N2CKO skin shows epidermal cysts replacing the follicle.

N2$^{flox/flox}$*; Msx2-Cre*/+ (N2CKO) mice were indistinguishable from wild-type (not shown). To ask if *Notch1* expression could compensate for the loss of *Notch2*, *N1*$^{flox/flox}$*; N2*$^{flox/flox}$*; Msx2-Cre*/+ (N1N2CKO) mice were analyzed. Like PSDCKO mice, N1N2CKO died around P25. Territories of bald, scaly skin, similar to those in PSDCKO mice, were observed (Figure 7B). Strikingly, histological examination revealed that *embryo-deleted* N1N2CKO skin resembled γ-secretase-deficient skin: hair follicles contained a melanin-producing core with large, loosely packed cells replacing the IRS (Figures 7C–7E, arrows); the ORS converted to the epidermal program after P12 and sebaceous glands were lost (Figure 7E and Supplemental Figure S3). Interestingly, *anagen-deleted* follicular morphology was normal at birth but became progressively worse as the animal aged, with most hair loss by P15 (Figures 7G–7I), suggesting that *anagen-deleted* follicles in N1N2CKO skin failed to maintain their structural integrity after onset of *Msx2-Cre* expression. In this respect, N1N2CKO follicles differed from their wild-type looking counterparts in PSDCKO skin. Histological examination of aged *anagen-deleted* N1N2CKO follicles confirmed these observations and revealed that by P25, instead of being in telogen (Figure 3E, arrow), they resembled the *embryo-deleted* follicles (Figure 7J). While the epidermis of N1N2CKO mice was hyperplastic, only the triple knockout mice (*N1*$^{flox/flox}$*; N2* $^{flox/flox}$*; N3* $^{-/-}$*; Msx2-Cre* or N1N2N3CKO) manifested frequent acanthotic and perakeratotic scales, identical to the PSDCKO mice (not shown).

Discussion

The specific *Cre* line we chose ensured complete deletion of the desired Notch allele(s) prior to the onset of dorsal skin morphogenesis at E9.5, an important experimental condition not accomplished previously. In further

contrast with the studies using *nestin-Cre* or tamoxifen-induced *Cre,* which generate a salt-and-pepper pattern of gene deletion (our unpublished observations with *K14-CreERT;ROSA26R* and the supplemental information in Yamamoto et al., 2003), *Msx2-Cre* generated mosaic animals with cells of identical phenotype forming a contiguous epithelium. This was fortuitous for several reasons. First, compound mice contain a mixed genetic background but mosaic clones permitted direct comparison of follicles with identical genetic background other than the deleted allele(s). Second, in addition to its early ectopic expression pattern, *Msx2-Cre* was expressed in all follicles after P1, thus providing an opportunity to compare the consequence of removing floxed alleles from different regions of the hair follicle (uniformly or only distally) and at different stages of hair development (before and after patterning of a hair follicle). In addition, mosaic animals generated by *Msx2-Cre* can present a unique opportunity to evaluate the behavior of stem cells with variable genetic makeup in the same organism by long-term studies.

Notch Proteins Cooperate to Regulate Epidermal Proliferation In Vivo

It was reported that Notch1 is required for withdrawal from the cell cycle of the basal epidermal keratinocytes (Rangarajan et al., 2001) and for commitment to epidermal differentiation of embryonic keratinocytes in tissue culture (Okuyama et al., 2004). However, we find a normal, differentiated epidermis formed after embryonic deletion of *Notch1*; it becomes slightly thicker than wild-type after birth (Supplemental Figure S3). Only compound loss of *Notch* genes or loss of γ-secretase resulted in deregulated epidermal proliferation. Postnatal loss of *Notch1* results in papilloma formation and tumors in aging mice (Nicolas et al., 2003), and single papilloma arose within the *embryo-deleted* N1CKO skin after 12 months. N1N3CKO and N1N2CKO animals were too young at the time of submission to observe papilloma formation, and PSDCKO animals die shortly after weaning. Transplantation of neonatal, *embryo-deleted PSDCKO; ROSA26R* skin to nude mice produced papilloma that were shed after 2–4 months, and no further outgrowth was detected. However, a few invasive, lacZ-positive nodules were observed (Y.P. and R.K., unpublished observation). This indicates that Notch signaling plays a dual role in long-term survival (required for growth or stem cell maintenance) and in tumor suppression (curtails growth, promotes differentiation). The mechanistic basis for these roles is under investigation.

Differentiation of Sebaceous Gland Is Affected by Alteration in Notch Signaling

Sebaceous glands are missing in the PSDCKO, N1N2CKO, and N1N2N3CKO mice and are severely reduced in N1CKO *embryo-deleted* skin. The hair germ was positive for the Val1744 antigen as early as E15.5 (Supplemental Figure S1; Lin and Kopan, 2003); thus, Notch signaling may be required to set aside sebaceous progenitors. However, we prefer the possibility that the impact on sebaceous development is an indirect consequence of epidermal and follicular abnormalities. Support for this interpretation is the observation that $N1^{-/-}$

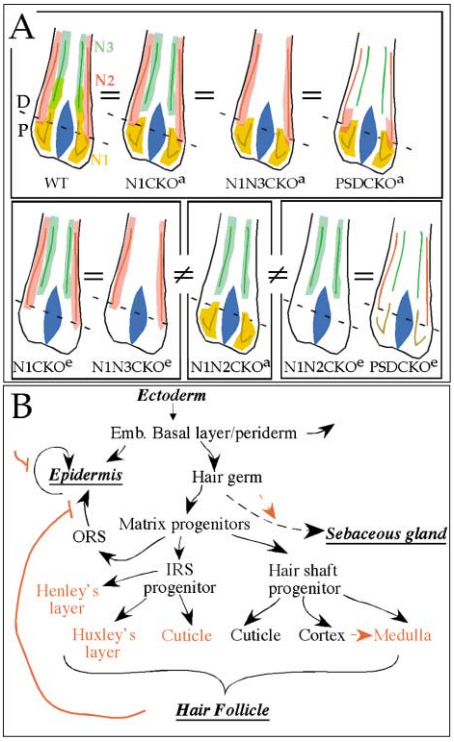

Figure 8. The Role of Notch Signaling in Mouse Skin

(A) Analysis of an allelic series of single and compound mutants of *Notch*- and *presenilin*-deficient follicles reveals a proximal (P) role for *Notch1* in the bulb and roles for *Notch1* and *2* in the distal (D) IRS. These activities are γ-secretase dependent. Notch mRNA/proteins are in colored lines; γ-secretase-dependent Notch activity is in diffused color. Superscript a, *anagen-deleted*; superscript e, *embryo-deleted*.

(B) Roles of Notch signaling (indicated in red) in epithelial skin lineages. Putative lineage relationships are indicated by black arrows. Dashed red arrow, nonautonomous or indirect role; affected hair layers are shown in red; inhibitory roles on epidermal conversion of ORS and on epidermal proliferation are also shown. See text for further details.

ES cells can form sebaceous glands in chimeric animals (Nichols et al., 2004) and that subcutaneous fat was reduced in the *embryo-deleted* N1CKO skin (Figure 6); this effect is indirect since *Msx2-Cre* is not active in the mesenchyme.

Essential Roles of Notch Signaling during Hair Follicle Morphogenesis

Notch genes are expressed in both proximal (*Notch1*) and distal (*Notch2* and *3*) cells (Figure 8A). *Notch2* overlaps with *Notch1* in the distal IRS, and *Notch3* overlaps with *Notch1* in the distal cortex (Figures 7A and 8A). Analyses of the mosaic animals generated by *Msx2-Cre* allowed us to uncover an essential, proximal function for *Notch1* in the bulb where it contributes to the medulla and the IRS (Henle's layer). This was supported by the observation that restoration of N1-NICD in all cortical cells distally failed to rescue the *embryo-deleted* follicles in *N1CKO; MHKA-NΔE* mice (Figure 5G and not shown; Lin et al., 2000). How does Notch1 activity in the proximal cortex impact the adjacent layers?

Notch1 mRNA is present in most cells of the proximal matrix but becomes restricted to the cortex and the cuticle layers (Kopan and Weintraub, 1993). We cannot rule out that activated Notch1, undetectable by the Val1744 antibody, was present in Henle's layer; however, no *Notch1* mRNA was detected in the medulla or its precursors in coat hair (Kopan and Weintraub, 1993; Powell et al., 1998). Therefore, while *Notch1* impact on Henle's layer may be direct (see below), *Notch1* regulates the medulla through a non-cell-autonomous mechanism (Figure 8B). Cell non-autonomous functions of *Notch* were described in the fly wing, where ectopic *Notch* activation can promote proliferation in adjacent cells (Giraldez and Cohen, 2003), and in the mouse nail (Lin and Kopan, 2003). In the fly wing, *Notch* loss acts cell non-autonomously, leading to loss of *Cut* expression in cells juxtaposed to *Notch*(-) clones across the margin (Micchelli et al., 1997). Interestingly, the mice deficient for mouse Cut (*Cutl1*) show defective IRS differentiation (Ellis et al., 2001). Thus, as in the fly wing, *Notch1* activation (even in one cortical cell; Lin et al., 2000) and *Notch1* loss (this report) produce subtle but distinct phenotypes in a neighboring cell, the medulla. The molecular nature of the non-cell-autonomous signal is under investigation.

A striking phenotype observed in the *embryo-deleted* PSDCKO and N1N2CKO follicles is their conversion into epidermal cysts. In wild-type skin, ORS cells can replenish the epidermis after injury; however, ORS does not respond during catagen or after hair depilation. This response may be controlled by an inhibitory signal produced by the hair follicle or a stimulating signal generated only by the injured tissue. The ORS of PSDCKO *embryo-deleted* follicles did not alter its proliferative rate (Figure 5D) until late anagen. At that time, *embryo-deleted* follicles either fail to produce this inhibitory signal or start to generate the stimulating one. As a result, ORS switches to the epidermal program during catagen. The resultant epidermal cyst resembles Nevus Comedonicus (NC), benign nevi believed to derive from a failure of the follicular/pilosebaceous unit to develop properly. NC are often associated with other developmental defects; at least one extensive case was reported in an individual with Alagille syndrome (Woods et al., 1994) caused by Jagged1 haploinsufficiency (Li et al., 1997; McCright et al., 2002). *Jagged1* expression overlaps with that of *Notch1* in the follicle (Favier et al., 2000; Powell et al., 1998). One explanation for the association between epidermal nevi and additional abnormalities was that a lethal autosomal mutation survives by mosaicism (Happle, 1991). Our observations are consistent with this suggestion: Nevus Comedonicus may be caused by mechanisms intrinsic to the epithelial compartment of the follicle, namely failure in Notch signaling or loss of its critical targets.

γ-Secretase Activity in Skin Is Mediated through Notch Signaling

A phenotype observed in the PSDCKO and N1N2CKO follicles is the failure to maintain the IRS and the subsequent loss of hair follicle. In the absence of all Notch signaling, cell fate selection proceeds normally with a correct radial symmetry. However, IRS cells seem most adversely affected by the loss of γ-secretase: although IRS cells (IRS 3.1-, GATA-3-, and trichohyalin-positive) form, they fail to accumulate. The few remaining cells are separated from each other (Figure 3J, arrows) and are replaced by the large, postmitotic cells seen between the ORS and the melanin-containing "shaft." Interestingly, a recent report suggests that Notch1 can activate *GATA-3* in CD4 T-helper cells (Amsen et al., 2004); perhaps a similar function for Notch signaling exists in the IRS.

Multiple Type I transmembrane proteins are substrates for γ-secretase. Independent from its role in γ-secretase, PS1 also contributes to Wnt signaling by targeting β-catenin for degradation (Kang et al., 2000; Soriano et al., 2001) and/or by impacting PI3K signaling (Baki et al., 2004). Can PSDCKO phenotypes be attributed to other activities or substrates of PS1? β-catenin-mediated PS1 effects manifest after months (Xia et al., 2001; our unpublished observations) while PSDCKO skin hyperproliferates in neonates. We did not detect significant changes in β-catenin expression within the affected hair follicles or the PSDCKO epidermis, suggesting that β-catenin is unlikely to contribute to the phenotypes. Instead, the striking similarity between the phenotypes of *embryo-deleted* hair follicles in N1N2CKO and PSDCKO mice, as well as the hyperproliferative, acanthotic, and perakeratotic epidermis of N1N2N3CKO and PSDCKO, strongly support the assertion that the primary target of PS in the skin is the Notch pathway. In addition, since inhibition of γ-secretase is a promising therapeutic approach for treatment of Alzheimer's disease, our results lessen the concerns that other γ-secretase substrates also play major signaling roles and provide evidence that the skin could act as a sentinel tissue for inhibitor-associated toxicity.

We find no evidence for γ-secretase-independent Notch activity, since *embryo-deleted* PSDCKO follicles containing Notch proteins (but no γ-secretase) are identical to follicles lacking *Notch* genes (N1N2CKO). The difference between *anagen-deleted* follicles of N1N2CKO and PSDCKO can be explained by the different consequences of removing substrate (Notch) versus protease (presenilin 1, 2). *Notch1* activity in the proximal matrix region may allow for normal follicular development in N2CKO, and *Notch2* activity in the distal IRS may compensate for loss of *Notch1* in N1CKO. In PSDCKO *anagen-deleted* follicles, PS1 mRNA and protein half-life determine how soon cells become depleted for γ-secretase activity (and thus NICD) along the proximo-distal axis. The distal activity of N2-NICD must have been maintained long enough to provide the required functions; we deduce this from the wild-type appearance of *anagen-deleted* PSDCKO follicles. In contrast, removal of the substrate (*Notch2*) within the same domain results in complete or earlier loss of N2-NICD; the residual proximal N1-NICD in N1N2CKO cannot maintain the follicular morphology, resulting in progressive deterioration of *anagen-deleted* N1N2CKO hairs (summary in Figure 8A).

In conclusion, our analyses of compound Notch mutants indicates that γ-secretase functions through Notch signaling in mouse skin and its epithelial appendages. *Notch* receptors act redundantly to control epithelial proliferation/differentiation and tissue homeostasis and

they are not required for patterning or for the initial specification/differentiation of the follicular cells (summary in Figure 8B). *Notch1* has an essential role in the proximal regions of hair follicles where it functions nonautonomously to affect the adjacent medulla and autonomously (with *Notch2*) in the IRS. Molecular mechanisms underlying these changes remain to be explored, but GATA-3 is a likely downstream effector for Notch signaling.

Experimental Procedures

Production and Analysis of Single and Compound Mutant Mice

The generation of conditional *Notch1* allele ($N1^{flox}$) (Yang et al., 2004), *Notch3* null (Leighton et al., 2001; Mitchell et al., 2001), and mice containing $PS1^{flox/flox}$; $PS2^{-/-}$ (Saura et al., 2004) were described previously; the *Notch2* conditional allele ($N2^{flox}$) will be described elsewhere.

N1CKO

$N1^{flox}/N1^{flox}$ females were crossed with *Msx2-Cre* males, and the F1 $N1^{flox/+}$; *Msx2-Cre*/+ male offspring were backcrossed to unrelated $N1^{flox}/N1^{flox}$ females. The F2 $N1^{flox/flox}$; *Msx2Cre*/+ mice displayed skin and hair phenotypes; all the other offspring ($N1^{flox/+}$; *Msx2-Cre*/+, $N1^{flox}/N1^{flox}$ or $N1^{flox/+}$) did not and were used as controls.

N2CKO

N2CKO were generated as N1CKO.

PSDCKO

$PS1^{flox/+}$; $PS2^{+/-}$; *Msx2-Cre*/+ males were crossed with $PS1^{flox/flox}$; $PS2^{-/-}$ females to produce compound mutant offspring ($PS1^{flox/flox}$; $PS2^{-/-}$; *Msx2-Cre*/+). ROSA26R reporter mice (Zambrowicz et al., 1997) and A7 transgenic line (Lin et al., 2000) were similarly bred into mice containing desired genotypes.

N1N2CKO

Female mice containing $N2^{flox}$ were crossed with $N1^{flox/flox}$; *Msx2Cre*/+ males to generate $N1^{flox/+}$; $N2^{flox/+}$; *Msx2-Cre*/+ male breeders, which then were crossed with $N1^{flox/flox}$; $N2^{flox/flox}$ females. The offspring $N1^{flox/flox}$; $N2^{flox/flox}$; *Msx2-Cre*/+ and its littermates were used for phenotypic analysis.

N1N3CKO

$N3^{-/-}$ females were similarly used to generate $N1^{flox/flox}$; $N3^{-/-}$; *Msx2-Cre*/+ for phenotypic analysis. Reagents and protocols used for PCR genotyping will be provided upon request.

Histology, In Situ Hybridization, BrdU Labeling, and Immunohistochemical Analysis

Skins/embryos were fixed in 4% paraformaldehyde in PBS, embedded in paraffin blocks, and sectioned at 5 μm. Sections were either subjected to hematoxylin/eosin staining, in situ hybridization, or the immunohistochemical analysis as previously described (Lin and Kopan, 2003; Lin et al., 2000). Digoxigenin-labeled antisense transcript for mouse *Notch2* (nucleotides 6437–7289; Acc. No. D32210) was detected by an anti-DIG antibody (Roche) coupled to alkaline phosphatase (AP) using BM purple AP substrate (Roche). For BrdU staining, mice were sacrificed 1–2 hr after injection for sample preparation. The source and dilution condition for primary antibodies including AE13, K17, S100A3, AE1, BrdU, and Ki67 refer to previous reports (Lin and Kopan, 2003; Lin et al., 2000). Other antibodies used include Filaggrin (rabbit, 1:1000; Covance), IRS3.1 (rabbit, 1:500; Porter et al., 2004), AE15 (mouse, 1:500; O'Guin et al., 1992), GATA-3 (mouse, 1:100; Santa Cruz, HCG3-31), and Cre (mouse, 1:100; Covance). When staining with mouse monoclonal antibodies, the MOM Basic kit (Vector Labs) was used. To stain sebocyte, fresh frozen samples were prepared and stained with a rabbit polyclonal antibody SCD-1 (1:500; Heinemann et al., 2003). Sections were counterstained with DAPI. AE15 was visualized by the metal-enhanced DAB substrate kit (Pierce).

Hair Hard Keratin Extraction and Western Blot Analysis

Hairs were clipped from the back skins of anesthetized 3-month-old N1CKO mice and their wild-type littermates. Keratins were extracted as described (Kopan and Fuchs, 1989) and loaded to SDS-PAGE after adjusting for protein concentration. Total proteins were visualized with Simple Blue (Invitrogen). K17 antibody was used at 1:2000 and AE 13 antibody at 1:10.

Oil Red-O, Whole-Mount X-gal Staining, and Electron Microscopy

Fresh, unfixed frozen samples were prepared and embedded in OCT, and 7 μm sections were prepared for Oil Red-O staining. For whole-mount X-gal staining, back skin were used as previously described (Kopan et al., 2002). For scanning EM, skin tissues were obtained from P9 *N1CKO* animals and control wild-type littermates, fixed in 2.0% glutaraldehyde, 2.5% paraformaldehyde, 0.1 M PBS (pH 7.4) at 25° for 1 hr, dehydrated, critical point dried, and visualized with a Hitachi S-2600H scanning electron microscope. For transmission EM, samples were fixed as above, dehydrated in an ethanol series followed by propylene oxide, and embedded in EMbed resin (Electron Microscopy Science). Ultrathin sections were cut with RMC MT-XL ultramicrotome, counterstained with Reynolds lead and uranyl acetate, and viewed with JEOL 100C TEM.

Acknowledgments

We would like to thank Dr. Kenji Kizawa (Kanebo Ltd., Japan) for the antibody against S100A3, Dr. Tung-Tien Sun (New York University) for the AE13 antibody, Dr. Rebecca Porter (University of Dundee, Scotland, UK) for the IRS 3.1 antibody, Dr. Pierre Coulombe (Johns Hopkins) for the K17 antibody, Dr. E. Koo for the S45 antibody, and Dr. Juris Ozols for the SCD1 antibody. We are also grateful to Drs. Marc Vooijs, Maxene Ilagan, and Malu Tansey for their critical comments on the paper, to Bill Coleman, Alma Johnson, and Marlene Scott for their technical assistance in making paraffin-embedded sections, and to Jamie Dant for performing the electron microscopy. $N3^{-/-}$ mice were kindly provided by Dr. Skarnes (University of California at Berkeley) and *Msx2-Cre* mice by Dr. Gail Martin (UCSF). R.K., M.-H.L., X.T., and Y.P. were supported GM55479-09, R.K., H.-T.C., and Y.P. were supported by HD044056-01, and T.G. was supported by NS036437.

Received: June 18, 2004
Revised: September 7, 2004
Accepted: September 13, 2004
Published: November 8, 2004

References

Allen, M., Grachtchouk, M., Sheng, H., Grachtchouk, V., Wang, A., Wei, L., Liu, J., Ramirez, A., Metzger, D., Chambon, P., et al. (2003). Hedgehog signaling regulates sebaceous gland development. Am. J. Pathol. *163*, 2173–2178.

Alonso, L., and Fuchs, E. (2003). Stem cells in the skin: waste not, Wnt not. Genes Dev. *17*, 1189–1200.

Amsen, D., Blander, J.M., Lee, G.R., Tanigaki, K., Honjo, T., and Flavell, R.A. (2004). Instruction of distinct CD4 T helper cell fates by different notch ligands on antigen-presenting cells. Cell *117*, 515–526.

Andl, T., Reddy, S.T., Gaddapara, T., and Millar, S.E. (2002). WNT signals are required for the initiation of hair follicle development. Dev. Cell *2*, 643–653.

Ashery-Padan, R., Marquardt, T., Zhou, X., and Gruss, P. (2000). Pax6 activity in the lens primordium is required for lens formation and for correct placement of a single retina in the eye. Genes Dev. *14*, 2701–2711.

Baki, L., Shioi, J., Wen, P., Shao, Z., Schwarzman, A., Gama-Sosa, M., Neve, R., and Robakis, N.K. (2004). PS1 activates PI3K thus inhibiting GSK-3 activity and tau overphosphorylation: effects of FAD mutations. EMBO J. *23*, 2586–2596.

Barrow, J.R., Thomas, K.R., Boussadia-Zahui, O., Moore, R., Kemler, R., Capecchi, M.R., and McMahon, A.P. (2003). Ectodermal Wnt3/beta-catenin signaling is required for the establishment and maintenance of the apical ectodermal ridge. Genes Dev. *17*, 394–409.

Braun, K.M., Niemann, C., Jensen, U.B., Sundberg, J.P., Silva-Vargas, V., and Watt, F.M. (2003). Manipulation of stem cell proliferation

and lineage commitment: visualisation of label-retaining cells in wholemounts of mouse epidermis. Development *130*, 5241–5255.

Chen, C.W., Jung, H.S., Jiang, T.X., and Chuong, C.M. (1997). Asymmetric expression of Notch/Delta/Serrate is associated with the anterior-posterior axis of feather buds. Dev. Biol. *188*, 181–187.

Cheng, H., Miner, J., Lin, M., Tansey, M.G., Roth, K.A., and Kopan, R. (2003). g-secretase activity is dispensable for the mesenchyme-to-epithelium transition but required for proximal tubule formation in developing mouse kidney. Development *130*, 5031–5041.

Crowe, R., Henrique, D., Ish-Horowicz, D., and Niswander, L. (1998). A new role for Notch and Delta in cell fate decisions: patterning the feather array. Development *125*, 767–775.

Ellis, T., Gambardella, L., Horcher, M., Tschanz, S., Capol, J., Bertram, P., Jochum, W., Barrandon, Y., and Busslinger, M. (2001). The transcriptional repressor CDP (Cutl1) is essential for epithelial cell differentiation of the lung and the hair follicle. Genes Dev. *15*, 2307–2319.

Favier, B., Fliniaux, I., Thelu, J., Viallet, J.P., Demarchez, M., Jahoda, C.A.B., and Dhouailly, D. (2000). Localisation of members of the notch system and the differentiation of vibrissa hair follicles: receptors, ligands, and fringe modulators. Dev. Dyn. *218*, 426–437.

Fuchs, E., and Raghavan, S. (2002). Getting under the skin of epidermal morphogenesis. Nat. Rev. Genet. *3*, 199–209.

Giraldez, A.J., and Cohen, S.M. (2003). Wingless and Notch signaling provide cell survival cues and control cell proliferation during wing development. Development *130*, 6533–6543.

Gridley, T. (2003). Notch signaling and inherited disease syndromes. Hum. Mol. Genet. *12* (*Suppl 1*), R9–R13.

Happle, R. (1991). How many epidermal nevus syndromes exist? A clinicogenetic classification. J. Am. Acad. Dermatol. *25*, 550–556.

Heinemann, F.S., Mziaut, H., Korza, G., and Ozols, J. (2003). A microsomal endopeptidase from liver that preferentially degrades stearoyl-CoA desaturase. Biochemistry *42*, 6929–6937.

Herreman, A., Hartmann, D., Annaert, W., Saftig, P., Craessaerts, K., Serneels, L., Umans, L., Schrijvers, V., Checler, F., Vanderstichele, H., et al. (1999). Presenilin 2 deficiency causes a mild pulmonary phenotype and no changes in amyloid precursor protein processing but enhances the embryonic lethal phenotype of presenilin 1 deficiency. Proc. Natl. Acad. Sci. USA *96*, 11872–11877.

Kang, D.E., Pietrzik, C.U., Baum, L., Chevallier, N., Merriam, D.E., Kounnas, M.Z., Wagner, S.L., Troncoso, J.C., Kawas, C.H., Katzman, R., and Koo, E.H. (2000). Modulation of amyloid beta-protein clearance and Alzheimer's disease susceptibility by the LDL receptor-related protein pathway. J. Clin. Invest. *106*, 1159–1166.

Kaufman, C.K., Zhou, P., Pasolli, H.A., Rendl, M., Bolotin, D., Lim, K.C., Dai, X., Alegre, M.L., and Fuchs, E. (2003). GATA-3: an unexpected regulator of cell lineage determination in skin. Genes Dev. *17*, 2108–2122.

Kopan, R., and Fuchs, E. (1989). A new look into an old problem: keratins as tools to investigate determination, morphogenesis, and differentiation in skin. Genes Dev. *3*, 1–15.

Kopan, R., and Ilagan, M.X.G. (2004). g-secretase: proteasome of the membrane? Nat. Rev. Mol. Cell. Biol. *5*, 7–12.

Kopan, R., and Weintraub, H. (1993). Mouse notch: expression in hair follicles correlates with cell fate determination. J. Cell Biol. *121*, 631–641.

Kopan, R., Lee, J., Lin, M.H., Syder, A.J., Kesterson, J., Crutchfield, N., Li, C.R., Wu, W., Books, J., and Gordon, J.I. (2002). Genetic mosaic analysis indicates that the bulb region of coat hair follicles contains a resident population of several active multipotent epithelial lineage progenitors. Dev. Biol. *242*, 44–57.

Krebs, L.T., Xue, Y., Norton, C.R., Sundberg, J.P., Beatus, P., Lendahl, U., Joutel, A., and Gridley, T. (2003). Characterization of Notch3-deficient mice: normal embryonic development and absence of genetic interactions with a Notch1 mutation. Genesis *37*, 139–143.

Kulessa, H., Turk, G., and Hogan, B.L.M. (2000). Inhibition of Bmp signaling affects growth and differentiation in the anagen hair follicle. EMBO J. *19*, 6664–6674.

Leighton, P.A., Mitchell, K.J., Goodrich, L.V., Lu, X., Pinson, K., Scherz, P., Skarnes, W.C., and Tessier-Lavigne, M. (2001). Defining brain wiring patterns and mechanisms through gene trapping in mice. Nature *410*, 174–179.

Li, L.H., Krantz, I.D., Deng, Y., Genin, A., Banta, A.B., Collins, C.C., Qi, M., Trask, B.J., Kuo, W.L., Cochran, J., et al. (1997). Alagille-Syndrome is caused by mutations in human Jagged1, which encodes a ligand for Notch1. Nat. Genet. *16*, 243–251.

Lin, M., and Kopan, R. (2003). Long-range, nonautonomous effects of activated Notch1 on tissue homeostasis in the nail. Dev. Biol. *263*, 343–359.

Lin, M., Leimeister, C., Gessler, M., and Kopan, R. (2000). Activation of the Notch pathway in the hair cortex leads to aberrant differentiation of the adjacent hair-shaft layers. Development *127*, 2421–2432.

Lowell, S., Jones, P., Le Roux, I., Dunne, J., and Watt, F.M. (2000). Stimulation of human epidermal differentiation by Delta-Notch signalling at the boundaries of stem-cell clusters. Curr. Biol. *10*, 491–500.

Lubman, O.Y., Korolev, S.V., and Kopan, R. (2004). Anchoring notch genetics and biochemistry; structural analysis of the ankyrin domain sheds light on existing data. Mol. Cell *13*, 619–626.

Ma, L., Liu, J., Wu, T., Plikus, M., Jiang, T.X., Bi, Q., Liu, Y.H., Muller-Rover, S., Peters, H., Sundberg, J.P., et al. (2003). 'Cyclic alopecia' in Msx2 mutants: defects in hair cycling and hair shaft differentiation. Development *130*, 379–389.

McCright, B., Lozier, J., and Gridley, T. (2002). A mouse model of Alagille syndrome: Notch2 as a genetic modifier of Jag1 haploinsufficiency. Development *129*, 1075–1082.

Meyers, E.N., Lewandoski, M., and Martin, G.R. (1998). An Fgf8 mutant allelic series generated by Cre- and Flp-mediated recombination. Nat. Genet. *18*, 136–141.

Micchelli, C.A., Rulifson, E.J., and Blair, S.S. (1997). The function and regulation of cut expression on the wing margin of *Drosophila*: Notch, Wingless and a dominant negative role for Delta and Serrate. Development *124*, 1485–1495.

Millar, S.E. (2002). Molecular mechanisms regulating hair follicle development. J. Invest. Dermatol. *118*, 216–225.

Mintz, B. (1971). Clonal basis of mammalian differentiation. Symp. Soc. Exp. Biol. *25*, 345–370.

Mintz, B., and Silvers, K. (1970). Histocompatibility antigens on melanoblasts and hair follicle cells. Transplantation *9*, 497–505.

Mitchell, K.J., Pinson, K.I., Kelly, O.G., Brennan, J., Zupicich, J., Scherz, P., Leighton, P.A., Goodrich, L.V., Lu, X., Avery, B.J., et al. (2001). Functional analysis of secreted and transmembrane proteins critical to mouse development. Nat. Genet. *28*, 241–249.

Mizutani, T., Taniguchi, Y., Aoki, T., Hashimoto, N., and Honjo, T. (2001). Conservation of the biochemical mechanisms of signal transduction among mammalian Notch family members. Proc. Natl. Acad. Sci. USA *98*, 9026–9031.

Nichols, A.M., Pan, Y., Herreman, A., Hadland, B.K., De Strooper, B., Kopan, R., and Huppert, S. (2004). The Notch pathway is dispensable for adipocyte specification. Genesis *40*, 40–44.

Nicolas, M., Wolfer, A., Raj, K., Kummer, J.A., Mill, P., Van Noort, M., Hui, C.C., Clevers, H., Dotto, G.P., and Radtke, F. (2003). Notch1 functions as a tumor suppressor in mouse skin. Nat. Genet. *33*, 416–421.

Niemann, C., Unden, A.B., Lyle, S., Zouboulis, C.C., Toftgard, R., and Watt, F.M. (2003). Indian hedgehog and {beta}-catenin signaling: role in the sebaceous lineage of normal and neoplastic mammalian epidermis. Proc. Natl. Acad. Sci. USA *100*, 11873–11880.

O'Guin, W.M., Sun, T.T., and Manabe, M. (1992). Interaction of trichohyalin with intermediate filaments: three immunologically defined stages of trichohyalin maturation. J. Invest. Dermatol. *98*, 24–32.

Okuyama, R., Nguyen, B.C., Talora, C., Ogawa, E., Di Vignano, A.T., Lioumi, M., Chiorino, G., Tagami, H., Woo, M., and Dotto, G.P. (2004). High commitment of embryonic keratinocytes to terminal differentiation through a Notch1-caspase 3 regulatory mechanism. Dev. Cell *6*, 551–562.

Porter, R.M., Gandhi, M., Wilson, N.J., Wood, P., McLean, W.H., and

Lane, E.B. (2004). Functional analysis of keratin components in the mouse hair follicle inner root sheath. Br. J. Dermatol. *150*, 195–204.

Powell, B.C., Passmore, E.A., Nesci, A., and Dunn, S.M. (1998). The Notch signalling pathway in hair growth. Mech. Dev. *78*, 189–192.

Radtke, F., Wilson, A., Stark, G., Bauer, M., van Meerwijk, J., MacDonald, H.R., and Aguet, M. (1999). Deficient T cell fate specification in mice with an induced inactivation of Notch1. Immunity *10*, 547–558.

Rangarajan, A., Talora, C., Okuyama, R., Nicolas, M., Mammucari, C., Oh, H., Aster, J.C., Krishna, S., Metzgers, D., Chambon, P., et al. (2001). Notch signaling is a direct determinant of keratinocyte growth arrest and entry into differentiation. EMBO J. *20*, 3427–3436.

Sauer, B., and Henderson, N. (1988). Site-specific DNA recombination in mammalian cells by the Cre recombinase of bacteriophage P1. Proc. Natl. Acad. Sci. USA *85*, 5166–5170.

Saura, C.A., Choi, S.Y., Beglopoulos, V., Malkani, S., Zhang, D., Rao, B.S., Chattarji, S., Kelleher, R.J., 3rd, Kandel, E.R., Duff, K., et al. (2004). Loss of presenilin function causes impairments of memory and synaptic plasticity followed by age-dependent neurodegeneration. Neuron *42*, 23–36.

Saxena, M.T., Schroeter, E.H., Mumm, J.S., and Kopan, R. (2001). Murine Notch homologs (N 1–4) undergo Presenilin dependent proteolysis. J. Biol. Chem. *276*, 40268–40273.

Schroeter, E.H., Kisslinger, J.A., and Kopan, R. (1998). Notch-1 signalling requires ligand-induced proteolytic release of intracellular domain. Nature *393*, 382–386.

Sengel, P. (1976). Morphogenesis of Skin (Cambridge: Cambridge University Press).

Slominski, A., Paus, R., and Costantino, R. (1991). Differential expression and activity of melanogenesis-related proteins during induced hair growth in mice. J. Invest. Dermatol. *96*, 172–179.

Soriano, P. (1999). Generalized lacZ expression with the ROSA26 Cre reporter strain. Nat. Genet. *21*, 70–71.

Soriano, S., Kang, D.E., Fu, M.F., Pestell, R., Chevallier, N., Zheng, H., and Koo, E.H. (2001). Presenilin 1 negatively regulates beta-catenin/T cell factor/lymphoid enhancer factor-1 signaling independently of beta-amyloid precursor protein and Notch processing. J. Cell Biol. *152*, 785–794.

Stenn, K.S. (2003). Molecular insights into the hair follicle and its pathology: a review of recent developments. Int. J. Dermatol. *42*, 40–43.

Sun, X., Lewandoski, M., Meyers, E.N., Liu, Y.H., Maxson, R.E., Jr., and Martin, G.R. (2000). Conditional inactivation of Fgf4 reveals complexity of signalling during limb bud development. Nat. Genet. *25*, 83–86.

Taylor, G., Lehrer, M.S., Jensen, P.J., Sun, T.T., and Lavker, R.M. (2000). Involvement of follicular stem cells in forming not only the follicle but also the epidermis. Cell *102*, 451–461.

Tournoy, J., Bossuyt, X., Snellinx, A., Regent, M., Garmyn, M., Serneels, L., Saftig, P., Craessaerts, K., De Strooper, B., and Hartmann, D. (2004). Partial loss of presenilins causes seborrheic keratosis and autoimmune disease in mice. Hum. Mol. Genet. *13*, 1321–1331.

Tumbar, T., Guasch, G., Greco, V., Blanpain, C., Lowry, W., Rendl, M., and Fuchs, E. (2004). Defining the epithelial stem cell niche in skin. Science *303*, 359–363.

Weng, A.P., and Aster, J.C. (2004). Multiple niches for Notch in cancer: context is everything. Curr. Opin. Genet. Dev. *14*, 48–54.

Woods, K.A., Larcher, V.F., and Harper, J.I. (1994). Extensive naevus comedonicus in a child with Alagille syndrome. Clin. Exp. Dermatol. *19*, 163–164.

Xia, X., Qian, S., Soriano, S., Wu, Y., Fletcher, A.M., Wang, X.J., Koo, E.H., Wu, X., and Zheng, H. (2001). Loss of presenilin 1 is associated with enhanced beta-catenin signaling and skin tumorigenesis. Proc. Natl. Acad. Sci. USA *98*, 10863–10868.

Yamamoto, N., Tanigaki, K., Han, H., Hiai, H., and Honjo, T. (2003). Notch/RBP-J signaling regulates epidermis/hair fate determination of hair follicular stem cells. Curr. Biol. *13*, 333–338.

Yang, X., Klein, R., Tian, X., Cheng, H.T., Kopan, R., and Shen, J. (2004). Notch activation induces apoptosis in neural progenitor cells through a p53-dependent pathway. Dev. Biol. *269*, 81–94.

Zambrowicz, B.P., Imamoto, A., Fiering, S., Herzenberg, L.A., Kerr, W.G., and Soriano, P. (1997). Disruption of overlapping transcripts in the ROSA beta geo 26 gene trap strain leads to widespread expression of beta-galactosidase in mouse embryos and hematopoietic cells. Proc. Natl. Acad. Sci. USA *94*, 3789–3794.

Zheng, Y., Eilertsen, K.J., Ge, L., Zhang, L., Sundberg, J.P., Prouty, S.M., Stenn, K.S., and Parimoo, S. (1999). Scd1 is expressed in sebaceous glands and is disrupted in the asebia mouse. Nat. Genet. *23*, 268–270.